



1 Spatiotemporal Source Apportionment of Ozone Pollution over the Greater 2 Bay Area

3 Yiang Chen¹, Xingcheng Lu^{2*}, Jimmy C.H. Fung^{1,3}

4 ¹ Division of Environment and Sustainability, The Hong Kong University of Science and Technology,
5 Clear Water Bay, Kowloon, Hong Kong SAR, China

6 ² Department of Geography and Resource Management, The Chinese University of Hong Kong, Sha
7 Tin, New Territory, Hong Kong SAR, China

8 ³ Department of Mathematics, The Hong Kong University of Science and Technology, Clear Water Bay,
9 Kowloon, Hong Kong SAR, China

10 *Correspondence to:* Xingcheng Lu (xingchenglu2011@gmail.com)

11

12 **Abstract.** It has been found that ozone (O₃) pollution episodic case is prone to appear when the Greater Bay Area
13 (GBA) is under the control of typhoons and sub-tropical high-pressure systems in summer. To prevent these
14 pollutions effectively and efficiently, it's essential to understand the contribution of O₃ precursors emitted from
15 different periods and areas under these unfavorable weather conditions. In this study, we further extended the
16 Ozone Source Apportionment Technology (OSAT) from the Comprehensive Air Quality Model with Extensions
17 (CAMx) model to include the function to track the emission periods of O₃ precursors. Then the updated OSAT
18 module was applied to investigate the spatial-temporal contribution of precursors emissions to the O₃
19 concentration over the GBA in July and August 2016, when several O₃ episodic cases appeared in this period.
20 Overall, the emissions within GBA, from other regions of Guangdong province (GDo), and the neighbouring
21 provinces are the three major contributors, which account for 23%, 15%, and 17% of monthly average O₃
22 concentration, respectively. More than 70% of O₃ in the current day is mainly formed from the pollutants emitted
23 within 3 days and the same day's emission contributed approximately 30%. During the O₃ episodes, when typhoon
24 approached, more pollutants emitted 2-3 days ago from the GDo and adjacent provinces were transported to the
25 GBA, leading to the increase of O₃ in this region. Under the persistent influence of northerly wind, the pollutants
26 originating from eastern China earlier than 2 days ago can also show an obvious impact on the O₃ over the GBA
27 in the present day, accounting for approximately 12%. On the other hand, the O₃ pollution is primarily attributed
28 to the local emission within 2 days when the GBA is mainly under the influence of the sub-tropical high-pressure
29 systems. These results indicated the necessity to consider the influence of meteorological conditions in
30 implementing the control measures. Meanwhile, analogous relationships between source area/time and receptor
31 were derived by the zero-out method, supporting the validity of the updated OSAT module. Our approach and
32 findings could offer more spatial-temporal information about the sources of O₃ pollutions, which could aid in the
33 development of effective and timely control policies.

34

35 1. Introduction

36 As one of the major air pollutants, ozone (O₃) is a secondary pollutant formed by the photochemical reactions of
37 nitrogen oxides (NO_x) and volatile organic compounds (VOCs) in the presence of solar radiation. The surface O₃
38 has detrimental effects on human health, such as causing respiratory and cardiovascular problems (Maji et al.,
39 2019; Yin et al., 2017). It could also lead to the reduction of crop yield and the damage of vegetation (Gong et al.,
40 2021; Wang et al., 2022c). With the implementing of a series of control policies in China since 2013, the
41 concentrations of other air pollutants, including particulate matter with aerodynamic diameters less than 2.5µm
42 (PM_{2.5}), NO_x, and sulfur dioxide (SO₂), have gradually decreased. In contrast, due to the large reduction of NO_x
43 emission and less control of VOCs emission in the early stage of the control period (Liu et al., 2023), the O₃
44 concentration still continuously increased and has become the major air pollutant across China. The Greater Bay
45 Area (GBA), including nine cities in the Pearl River Delta (PRD) region, Hong Kong (HK), and Macau Special
46 Administrative Regions (SAR), is one of the most developed agglomerations in China and also facing with the
47 heavy O₃ pollution problem. Based on the analysis of surface monitor observation, Cao et al. (2024) and Feng et



48 al. (2023) found that the daily maximum 8hr average (MDA8 O₃) in the PRD region and HK showed an overall
49 upward trend by 1.11 and 0.22 ppbv/year from 2013 to 2019 and from 2011 to 2022, respectively.

50 The formation of O₃ is closely related to the source of its precursors and much effort has been devoted to
51 investigating the source region and source category of O₃ in the GBA using different methods (Liu et al., 2020a).
52 He et al. (2019) applied the positive matrix factorization (PMF) method to resolve the anthropogenic sources of
53 VOCs. Combining with a photochemical box model with the master chemical mechanism (PBM-MCM), they
54 found that vehicular was the most significant source to the O₃ formation, followed by biomass burning and solvent
55 usage. Li et al. (2012) applied the CAMx-OSAT numerical model to track the source contribution to O₃ in the
56 GBA region and found that elevated local and regional contribution is dominant under the O₃ episodes. Yang et
57 al. (2019b) applied the NAQPMS model with an on-line source apportionment module to explore the source of
58 O₃ in different seasons in the PRD region. Their results shows that the mobile is the largest contributor, followed
59 by industry. Fang et al. (2021) used multi-modelling source apportionments to quantify the source impact on O₃
60 in the PRD region. The on-road mobile and industrial process were found as two major contribution sections.
61 Integrating satellite data and sensitivity model simulations, Wang et al. (2022a) found that enhanced biogenic
62 emission and cross-regional transport by approaching typhoons are significant factors lead to the ozone pollution
63 in the PRD and Yangtze Rivel Delta (YRD) regions. In addition to the source region and category, emitting time
64 of pollutants is also an important perspective that needs to be better understood for effective and efficient control
65 policymaking. Some studies have attempted to evaluate this temporal perspective (Xie et al., 2021; Ying et al.,
66 2021). Xie et al. (2023) analysed the age evolution of PM_{2.5} during a haze event in eastern China. It showed that
67 during the regional transport stage, more aged particles from the North China Plain (NCP) were transported to the
68 downwind YRD region and leading to a sharp increase in the average age of different components of PM_{2.5} in
69 YRD. Chen et al. (2022c) analyses the temporal contributions of emissions to the concentration of PM_{2.5} in the
70 PRD region and found that pollutants emitted from 2 days earlier were trapped within the PRD region due to the
71 weak wind during the episodic pollution. However, these studies mainly focus on the PM_{2.5} and the temporal
72 contribution of sources to the O₃ in the GBA region still remain unclear.

73 Besides emission, the meteorological condition, another key factor that can affect the transportation, production,
74 and destruction of O₃ and its precursors, also received much attention and has been extensively studied (Lu et al.,
75 2019; Wang et al., 2017; 2022b). The long/short-term effects of changes in meteorological conditions on ozone
76 concentrations have been investigated through a variety of methods, such as statistical analysis of observations
77 and numerical modelling (Yang et al., 2019a; Xu et al., 2023a; Zheng et al., 2023). Liu and Wang (2020b)
78 conducted sensitivity simulations by the CMAQ model to evaluate the contribution of weather condition variation
79 to summer O₃ levels from 2013-2017. Their results show that the meteorological conditions were more conducive
80 to ozone formation from 2014 to 2016 than in 2013, and it can lead to an increase of more than 10 ppbv in MDA8
81 O₃ in Guangzhou. Different objective and subjective classification technologies have been applied to summarize
82 the impacts of unfavorable weather patterns on O₃ pollution (Han et al., 2020; Chen et al., 2022b; Cao et al., 2023).
83 Gao et al. (2018) summarized the commonly synoptic patterns in the Guangdong province that O₃ pollution always
84 occurred and concluded that the sub-tropical high-pressure system and typhoons are two major patterns accounting
85 for more than 60% in the PRD regions during 2014 – 2016. The major influence factor and the dominant
86 contributed physical and chemical process were also identified and analyzed (Gong et al., 2022; Zeren et al., 2022;
87 Wu et al., 2023). Ouyang et al. (2022) analysed the impact of a subtropical high and a typhoon on ozone pollution
88 in the PRD region and found that low relative humidity, high boundary layer height, weak northerly surface wind,
89 and strong downdrafts were the main meteorological factors contributing to the pollution. Deng et al. (2019)
90 illustrated that the actinic flux is the important cause of the co-occurrence of high ozone and aerosol pollution
91 under the control of typhoon periphery. Li et al. (2022) also investigated the impact of peripheral circulation
92 characteristics of typhoons and found that the chemical formation and vertical mixing effects are two major
93 contributors to the enhancement of O₃ levels, while the advection showed negative values. Qu et al. (2021)
94 analysed the typhoon-induced and non-typhoon O₃ events in the PRD region and revealed that under the influence
95 of typhoons, the contributions from the transport processes and sources outside the PRD increased. Usually, the
96 ozone events are attributed to changes in meteorological conditions rather than sudden increases in emission
97 intensity (Lin et al., 2019; Xu et al., 2023b). The change of weather conditions will affect the time-sensitivity of
98 emitted pollutants and lead to different types of O₃ pollution that can result from long-range transport of elder
99 pollutants or accumulation of local fresh pollutants. Hence, it's of great importance to clarify the impact of the
100 pollutants from different source areas and emitting periods on the O₃ pollution under different weather conditions
101 in the GBA.

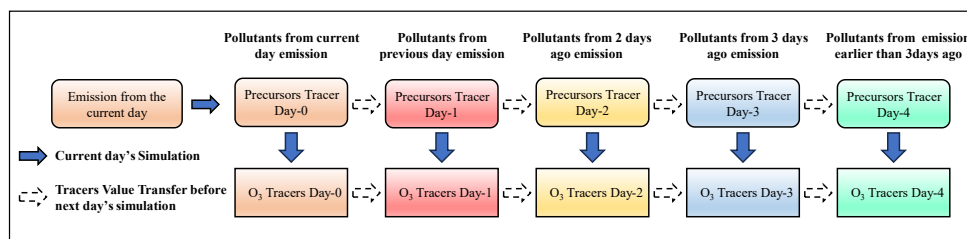


102 In this study, the CAMx-OSAT model was extended and used to track the temporal contribution of pollutants to
 103 the O₃ pollutions over the GBA under the impact of typhoons and sub-tropical high pressure during July and
 104 August in 2016, the two most important weather system that influence O₃ pollutions over the GBA. The rest of
 105 this paper is organized as follow. The temporal source apportionment (TSA) method, the configuration of
 106 experiments, and the ozone episodes were introduced in section 2. The spatial-temporal source apportionment
 107 results and zero-out simulation results were shown and discussed in section 3. The major conclusions were
 108 summarised in section 4.

109 2. Methodology and Data

110 2.1 Temporal Source Apportionment Method

111 Previously, we have successfully implemented the PM_{2.5} temporal source apportionment (TSA) method in the
 112 Comprehensive Air Quality Model with Extensions (CAMx) model and applied it to investigate the temporal
 113 influence of emissions on PM_{2.5} in the GBA (Chen et al., 2022c). Here, we further extend this method to track the
 114 temporal contribution of emissions to O₃ and its precursors. The basic mechanism of the TSA method is to track
 115 the contribution of pollutants from different emitting periods using a set of tracers. In the TSA method (Fig. 1),
 116 the *Precursor Tracer Day-x* was used to track the precursors emitted from *x* days ago. The *O₃ Tracer Day-x* was
 117 used to track the O₃ formed from the precursors emitted from corresponding *x* days ago (namely *Precursor Tracer*
 118 *Day-x*). The tracers in *Day-x* can be set into different finer periods (e.g., every 1 hour, 6 hours, 24 hours) as
 119 required. The total tracer number will be decided according to the whole tracking period and the minimum tracking
 120 period per tracer. For instance, if the whole tracking period is 5 days and the minimum tracking period per tracer
 121 is every 6 hours, the total tracer number will be 20. As shown in the Figure 1, during each day's simulation,
 122 the contribution of present day's emission will always be tracked by the Day-0 tracers. After completing the current
 123 day's simulation and before starting the next day's simulation, each tracer *Day-x*'s value transfers to the
 124 corresponding tracer *Day-(x+1)*, which represents one day earlier than *Day-x*, in the following sequence. For
 125 example, beginning from the penultimate tracer, namely values in Day-3 transfer and add into Day-4, then the
 126 values in Day-2 transfer to Day-3, followed by Day-1 to Day-2, and lastly Day-0 to Day-1 (Dash arrow in Figure
 127 1). Here, the value in Day-3 tracer will add into the last tracer (Day-4) because the last tracer represents the total
 128 contribution of pollutants emitted earlier than 3 days ago. More details of this method can be found in Chen et al.
 129 (2022c).



130

131 Figure 1. Schematic diagram of temporal source apportionment (colors represent the pollutants released or formed
 132 by emissions on different days).

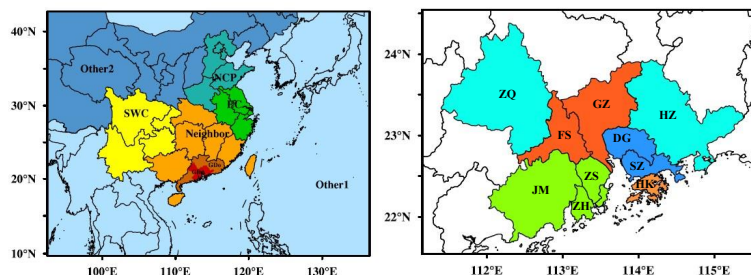
133 2.2 Model Configuration and Evaluation

134 The Weather Research and Forecasting (WRFv3.9) model was applied for meteorological field simulation. The
 135 initial and boundary condition for WRF model was gained from the Final Operational Global Analysis data (FNL).
 136 The CAMx v7.1 was used to simulate the spatial-temporal variation of air pollutants. The initial and boundary
 137 condition for CAMx model was provided by the Model for Ozone and Related chemical Tracers, version 4
 138 (MOZART-4). Regarding the emission, a highly resolved emission inventory provided by Hong Kong
 139 Environmental Protection Department was used for the GBA region, and the Multi-resolution Emission Inventory
 140 for China (MEIC, Li et al., 2017) developed by the Tsinghua University was applied for the area outside the GBA
 141 region. The biogenic emission was calculated the Model of Emissions of Gases and Aerosols from Nature
 142 (MEGAN version 3.1). The CB05 gas phase chemistry, the ISORROPIA inorganic aerosol scheme and the SOAP
 143 secondary organic aerosol scheme were used in the simulation. This model system has been applied to analyse the



144 source of O_3 , NO_x and $PM_{2.5}$ in the GBA region in the previous studies (Lu et al., 2016; Chen et al., 2022a; Chen
145 et al., 2022c). More configuration of this model system can refer to the work of Lu et al. (2016).

146 The three-nested simulation domain of the WRF-CAMx model was shown in Figure S1. The resolution of three
147 domains was 27km, 9km, and 3km, respectively. For the source apportionment experiments, the simulation
148 domain was divided into 12 source regions as shown in Figure 2, including North China Plain (*NCP*), eastern
149 China (*EC*), southern western China (*SWC*), other regions of inland China (*Other 2*), ocean and other countries
150 (*Other 1*), neighbouring provinces around Guangdong province (*Neighbor*), Other region within Guangdong
151 province (*GDo*), Guangzhou and Foshan (*GF*), Shenzhen and Dongguan (*SD*), Hong Kong (*HK*), Zhuhai,
152 Zhongshan and Jiangmen (*ZZJ*), Zhaoqing and Huizhou (*GBAo*). The cities within the GBA were separated into
153 different sub-regions mainly based on their geographical location, same as the work of Chen et al. (2022c). Since
154 the source contribution to the O_3 in Zhaoqing and Huizhou is relatively different with that of their neighboring
155 cities (Chen et al., 2022a), these two cities were grouped into one sub-region. The contribution of initial and D1
156 boundary conditions were also treated as two sources. In the following analysis, for the O_3 concentrations in the
157 target area over the GBA, the influence of pollutants emitted within the target area is treated as the local
158 contribution, and the influence of pollutants originating from the other areas within the GBA region is treated as
159 the regional contribution. The source tracking time period is 5 days (Day-0, Day-1, Day-2, Day3 represent the
160 pollutants emitted within the present day, the previous day, two days ago, and three days ago, respectively. Day-4
161 the total contribution of pollutants emitted earlier than three days ago). The simulation period is July and August
162 2016, and the model was spin-up for 7 days to reduce the influence of initial condition.



163

164 Figure 2. The configuration of source areas in the source apportionment experiments (One color represents one
165 source area. The GBA source were divided into five source areas. *Other 1* represents ocean and other countries.
166 *Other 2* represents other area within the mainland China in the simulation domain.)

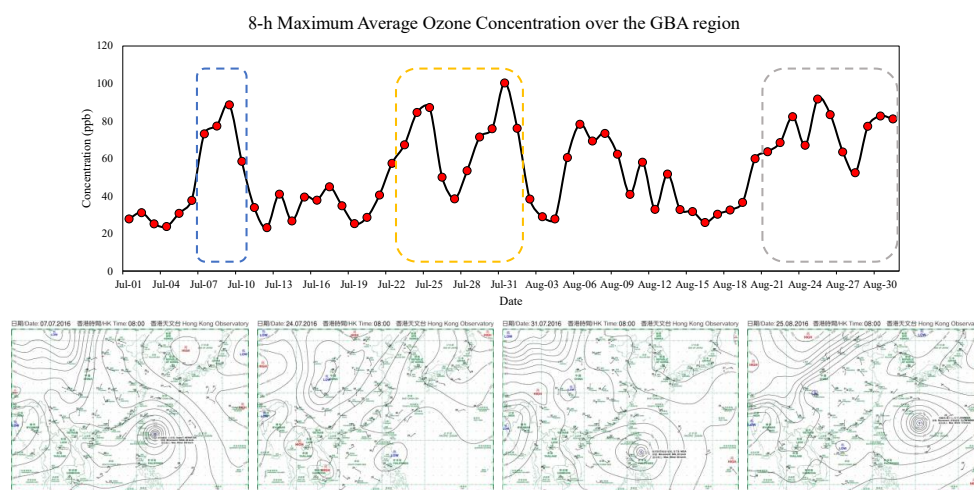
167 The performance of simulated 2-m temperature, 10-m wind speed, and O_3 concentration were evaluated and
168 shown in Table S1. The recommended values suggested by Emery et al. (2001) and EPA (2007) were used as
169 benchmark and shown in the brackets in Table S1. The temperature was a little overestimated with a mean bias
170 (MB) of 0.33, while the wind speed was underestimated with MB of -0.45. The index of agreement (IOA) was
171 0.82 and 0.70 for temperature and wind speed, respectively. The MBs and IOAs both fulfilled the criteria. But the
172 root mean square error (RMSE) show a little higher than the value of criteria. Regarding the O_3 , the IOA reach
173 0.81. The small positive MB indicated that the model slightly overestimated the O_3 concentration. The normalized
174 mean bias (NMB) is 0.13, which also meet the criteria. The time series comparison (Fig. S2) of average O_3
175 concentration in Guangzhou, Hong Kong and Zhuhai illustrates that the model can well catch and reproduce the
176 variation trend of O_3 concentration in GBA, although there is a few difference between the simulated and measured
177 concentration for some peaks, like the period between 25 July and 31 July in Guangzhou. Overall, the performance
178 of model simulation is comparable to the other studies in this region (Li et al. 2022; Yang and Zhao, 2023).
179 Therefore, the simulation result is reasonable and can be further used for source analysis.

180 2.3 Ozone Episodes

181 There were several O_3 episodes occurred during the simulation period. Here, the 8-h maximum O_3 concentration
182 (MDA8) over the GBA was calculated using the observation data from the surface monitors stations (Fig. 3). The
183 first O_3 pollution occurred between the 7th and 10th of July (Ep1). During this period, the GBA region was firstly
184 controlled by the sub-tropical high-pressure system. When the typhoon north-westerly moved from the east sea
185 area of the Philippines to Taiwan province, the GBA was located in the peripheral subsidence region. After the



186 typhoon made landfall, the high-pressure situation in the GBA was relieved and the O₃ concentration decreased.
187 There were another two O₃ episodes between 24 July and 1st August. The GBA was mainly influenced by the sub-
188 tropical high-pressure system during 24th-26th July (Ep 2), while the synoptic condition of GBA between 30th July-
189 1st August (Ep3) was similar to that of Ep1. During the Ep3 period, there was another typhoon moving north-
190 westerly from the east sea area of the Philippines and influencing the GBA region. It was found that this type of
191 typhoon movement path was often accompanied by the occurrences of O₃ pollution in the GBA (Wang et al.,
192 2022a). In late August, under the joint influence of the subtropical high-pressure system and the typhoon, the O₃
193 over the GBA maintained a high concentration level between the 21st -31st of August (Ep4). Unlike the moving
194 paths of the previous two typhoons, this typhoon was moving southerly from the sea areas south of Japan and
195 stayed near the sea areas east of Taiwan province. The typhoon moved north after 27th August, and northerly winds
196 prevailed in the GBA. Hence, we conducted the simulation of O₃ concentration in the GBA during July-August
197 2016 and analysed the spatiotemporal contributions of emissions in these episodic cases.



198
199 Figure 3. The time-series of the MDA8 O₃ concentration over the GBA during July-August 2016 and the
200 synoptic patterns during the O₃ episodes. (The weather charts were downloaded from the Hong Kong
201 Observatory; <https://www.hko.gov.hk/en/wxinfo/currwx/wxcht.htm>)

202

203 3. Result and Discussion

204 3.1 Source Area Contributions

205 The contribution of different source areas to the average O₃ in the GBA region was shown in Table 1. Here, the
206 contribution from initial and boundary condition were treated as background contribution. Regarding the monthly
207 average O₃ concentration over the GBA region, the emission within the GBA can contribute about 23%. The
208 pollutants from other regions within Guangdong Province (GDo) and neighbouring provinces also have large
209 contribution, accounting for approximately 15% and 17%, respectively. Under the influence of prevailing south
210 winds in the summertime, the contribution from ocean and other countries can also account for about 20%. As
211 some studies suggested that O₃ originating from foreign countries is quite limited (Sahu et al., 2021), the main
212 contributor of this source is likely to be marine ship emissions from ocean. The pollutants from other source
213 regions have limited effect on the O₃ in the GBA.

214 The monthly average source area contribution to four sub-regions within the GBA region can be found in Table
215 S2. Results shows that the local emission has large influence on O₃ in GF and SD regions, accounting for 17% of
216 O₃ but it has impact lower than 10% on O₃ in ZZJ region and HK city. The contribution of GBA regional emission
217 (contributed by other GBA tagged regions) has a relatively larger impact to the monthly average O₃ concentration
218 in GF region than the other sub-regions. It's because the prevailing southerly wind in summer, so the pollutants
219 within the GBA region have a large influence on O₃ in GF area. The influences of pollutants from GDo and



220 neighboring to different subregions ranges from 25% to 31%. As the coastal regions, the ZZJ region and HK city
 221 also suffer more from sources of ocean and other countries, which occupied about 24% and 27%.

222 Regarding the average O₃ concentration over the GBA region in different episode periods, it can be found that,
 223 during the typhoon episodes (i.e., Ep1, Ep3 and Ep4), the contribution of non-local emission has increased. The
 224 typhoon paths are quite similar in the Ep1 and Ep3 episodes (Fig. S3). Results show that the total contribution of
 225 GDo and neighbouring provinces have increased and reached more than 50% for O₃ over the GBA in these two
 226 typhoon episodes. As shown in Figure S4, with the approaching of typhoon, the wind speed increased and the
 227 average wind direction over the GBA changed from south to north. Therefore, more pollutants from the
 228 surrounding provinces were transported to GBA. Considering the typical circulation of typhoon periphery (Figure.
 229 S4 and S6), it was judged that more pollutants may come from Jiangxi, Fujian, and Hunan provinces. During the
 230 Ep1 and Ep3 episodes, the contribution of local emission in different sub-regions slightly decreased. With the
 231 change of the wind direction from south to north in these two periods, the influence of pollutants within GBA to
 232 O₃ in GF area decreased from 15% to 8%. The contribution of GBA emission to the O₃ in other sub-regions
 233 increased, especially the ZZJ area and HK city. It is because with the change of wind direction, these two regions
 234 were located at the downwind area of the GF and SD regions, which are the emission hotspots within the GBA.
 235 At the same time, the contribution of source from ocean and other countries also decreased approximately 10%.
 236 The influence of GDo and neighbouring provinces increased 27%, 21%, 32% and 22% for GF, SD, ZZJ regions
 237 and HK city, respectively.

238 In another typhoon process (Ep4), where the typhoon's moving path differed from the other two typhoon cases,
 239 there was an increase in contribution from GDo and neighbouring provinces under the influence of persistent
 240 northerly wind. Furthermore, it was observed that pollutants from eastern China (EC) and North China Plain (NCP)
 241 could also influence the O₃ levels in the GBA, accounting for approximately 12%. Similar increases in the impact
 242 of emissions from the EC and NCP were also found in the four sub-regions.

243 In the Ep2, the GBA was mainly controlled by the sub-tropical high-pressure system and southerly wind still
 244 prevailed. However, the wind speed was low and conducive to the accumulation of the pollutants. Hence, the local
 245 sources were the dominant contributor and accounting for about 44% but the contribution from GDo and
 246 neighboring provinces decreased. For O₃ in the GF region, as discussed above, the O₃ in the GF regions is more
 247 susceptible to emissions within the GBA under the prevailing southerly wind. Thus, not only the local contribution
 248 but also the GBA regional contribution largely increased in the GF region. The regional contribution is larger in
 249 the GF region, increasing from 15% to 33%. For the other sub-regions, the main increase was in local contributions.

250

251 Table 1. Contribution of pollutants from different source areas to the O₃ concentration over the GBA in different
 252 cases.

Case	GBA	GDo	Neighbor	Other 1	EC	SWC	NCP	Other 2	Background
Monthly	23%	15%	17%	20%	3%	1%	1%	1%	20%
Ep1	18%	21%	35%	10%	3%	0%	0%	0%	13%
Ep2	44%	11%	7%	27%	0%	0%	0%	0%	11%
Ep3	19%	34%	25%	9%	3%	0%	1%	1%	9%
Ep4	20%	16%	18%	15%	8%	1%	4%	3%	14%

253 * Here, *GDo* represents areas outside the GBA but within Guangdong province. *Neighbor* represents the provinces around
 254 Guangdong province. *Other 1* represents ocean and other countries. *Other 2* represents other areas within the mainland China
 255 in the simulation domain. *Background* represents the contribution of initial and boundary conditions.

256 3.2 Emission Period Contributions

257 The contribution of pollutant emitted from different time periods to the average O₃ in the GBA and sub-regions
 258 was shown Figure. 4 and Table. S3. The background contribution was not considered in the temporal source
 259 contribution analysis. This is because the background contribution is primarily derived from boundary conditions,
 260 and its temporal contribution was calculated based on the time when the pollutants were transported into D1 rather
 261 than the actual emission time.

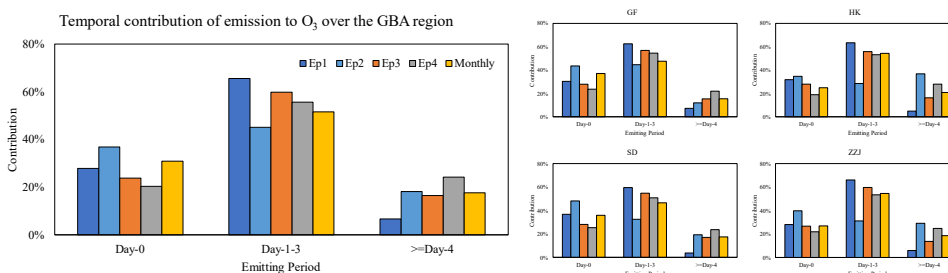


262 Overall, under the general monthly condition, the emission within 3 days (namely from Day-0 to Day-2) account
263 for approximately 73% of monthly average O₃ concentration within GBA. The largest proportion of O₃, around
264 31%, formed from the current day's emission (Day-0) and the contribution of pollutants from earlier emission
265 periods decreases as time increases. For the monthly average O₃ in different sub-regions, more O₃ in GF and SD
266 regions was formed from the emission from Day-0, which contributed about 37% and 36%, respectively. The
267 contribution of emissions from Day-1 decreased to about 23% in these two regions. The contribution of Day-0
268 and Day-1 emissions was relatively small but stable for HK city and ZZJ region, which account for around 25%
269 and 27%, respectively. The influence of pollutants emitting earlier than 3 days ago (i.e., Day-4) is mostly lower
270 than 20%.

271 The situations are different during the pollution periods. The contribution of emission from the current days to the
272 average O₃ over the GBA both decreased in two typhoon cases with similar moving path (Ep1 and Ep3), but the
273 contribution of emissions from Day-1 to Day-3 increased 14% and 8%, respectively. And the influence of
274 pollutants emitted earlier than 3 days ago (\geq Day-4) decreased 11% in Ep1 and almost no change in Ep3. This
275 indicates that these two ozone pollutions were caused by the accumulation of pollutants within the current 3 days.

276 For another typhoon case (Ep4), the contribution from the Day-0 decreased approximately by 11%, comparing
277 with the monthly contribution over the GBA. At the same time, the influence of pollutants from earlier emitting
278 period increased, especially for those earlier than 3 days ago (Day-4). It means that the O₃ pollution for this period
279 is a persistent pollution process. The major contributor should not only the local emission, but also the long-range
280 transport. Similar variation trend of the temporal contributions of emission to different sub-regions can be
281 concluded, which also illustrated that the O₃ pollution is usually a regional problem.

282 For Ep2, the contribution of emissions from Day-0 increased approximately 18%, while the influence of Day-1-
283 3's emissions decreased about 18%. According to the source area contribution result, the source area of O₃ over
284 GBA in Ep2 is mainly local sources. So the contribution of the freshly emitted pollutants was larger. The
285 contribution of Day-4 emissions to HK and ZZJ regions in Ep2 is larger. It is probably because the prevailing
286 south wind direction brought more airflow came from the ocean. Compared with the emission of GF and SD
287 regions, HK city and ZZJ region have lower emission amounts. At the same time, HK city and ZZJ region locate
288 in the upwind region, and the pollutants from GBA would have a smaller influence on the O₃ in these two regions.
289 Hence the fresh pollutants amount was smaller and contributed similarly to the Day-4 emissions, which is an
290 accumulated amount.



291

292 Figure 4. Contribution of pollutants from different emitting periods to the O₃ concentration over the GBA in
293 different cases.

294

295 3.3 Source Area-Time Contributions

296 To further clarify the relationship between sources and the O₃ concentration of target regions, the evolution of O₃
297 from various source areas and periods were analyzed. Figure 5 shows the time series of the contributions from
298 different source areas and precursors emission periods for the average O₃ concentration in the GBA region.

299 Regarding the monthly average O₃ concentration over the GBA, the emissions within the GBA is the major
300 contributor and generally have a larger effect in the current day. Under the control of southerly wind, as shown
301 in Figure 6, the pollutants emitted 1 day ago (Day-1) were gradually transported out of the GBA, and the influence



302 of the GBA's emission earlier than Day-1 is much lower. At the same time, the pollutants of GDo and neighboring
303 provinces emitted 1 day ago began to have impact on the O₃ in the GBA. However, the elder pollutants from GDo
304 and neighboring provinces cannot greatly influence on the O₃ in the GBA due to the prevailing southerly wind.

305 However, regarding the O₃ pollution between 7th and 10th July (Ep1), the major contributors changed. On 7th July,
306 the GBA was under the control of the subtropical high system, and the typhoon was located near the east of Taiwan
307 province. The weather condition was unfavourable for pollutants dispersion, and the O₃ sourced from Day-1
308 emission within Guangdong provinces was trapped. The prevailing wind shifted to northerly wind, and it also
309 brought some elder pollutants from neighboring provinces to the GBA. With the approach of the typhoon on 8th –
310 10th July, although stronger northwest wind speeded up the diffusion of pollutant from GBA and decreased the
311 local contribution, it also transported more elder pollutants from the northern inland to the GBA. It can be found
312 that the emission from GDo in the present day also had a significant contribution. At the same time, the pollutants
313 from the neighboring provinces dominated the Day-1 to Day-3 emissions. Moreover, the pollutants emitting 2
314 days ago in the eastern China (EC) region were also transported southerly and affected on the O₃ of GBA in the
315 current day. Figure 7 shows the spatial distribution of average source contribution during the Ep1 period.
316 Compared with the monthly average (Figure 6), it was found that the elder pollutants originating from the GBA
317 can be transported back and influence the O₃ concentration in the western part of GBA during the Ep1 period.
318 This is because easterly and east winds blew over the GBA from 5th-6th July (Before Ep1, Figure S4). The
319 pollutants emitted within the GBA were transported to northwest inland. However, under the influence of
320 northwest wind, they were transported back to the GBA again. It can also be seen that the pollutants from the GDo
321 1 day ago were transported downwind quickly, contributing to a high O₃ concentration over the Pearl River Estuary.
322 According to the wind pattern, they mainly came from the northern and western parts of the Guangdong province.
323 Meanwhile, the neighboring provinces' emissions from Day-1 to Day-3 were also transported to the GBA with
324 the northwest wind, continuously affecting the O₃ over this region.

325 For the Ep3 O₃ pollution process, results show that the pollutants from GDo and neighboring provinces were also
326 the major contributors. From 30th– 31st July, the GBA was under the control of high pressure, and it blew weak
327 north wind in this region. Afterward, the approaching of typhoon (1st August) further strengthened the cross-
328 regional transport of pollutants. The difference between Ep3 and Ep1 is that the emissions from GDo have a larger
329 impact on the Day-1 and Day-2 emissions. Additionally, while pollutants from neighboring provinces and EC in
330 Day-4 emission only accounted for about 5ppb in Ep1, they can still contribute to about 10ppb in Ep3. The possible
331 reason is that northerly wind prevailed over Fujian, Jiangxi, and Hunan provinces during the whole Ep1 period
332 (Figure S4), while easterly wind still blew over these provinces during the earlier period of the Ep3 (30th– 31st
333 July, Figure S6), which slowed the transport and influence of pollutants from the neighboring provinces. Generally,
334 the pathways of typhoons in the Ep1 and Ep3 episodes were quite similar, and the influence regions of typhoon
335 wind field mainly cover Guangdong and neighboring provinces. Therefore, the major source area and source time
336 are quite similar in these two cases. To prevent this type of O₃ pollution, earlier emission control (at least 3 days
337 ago) and collaboration with neighboring provinces will gain a better control result.

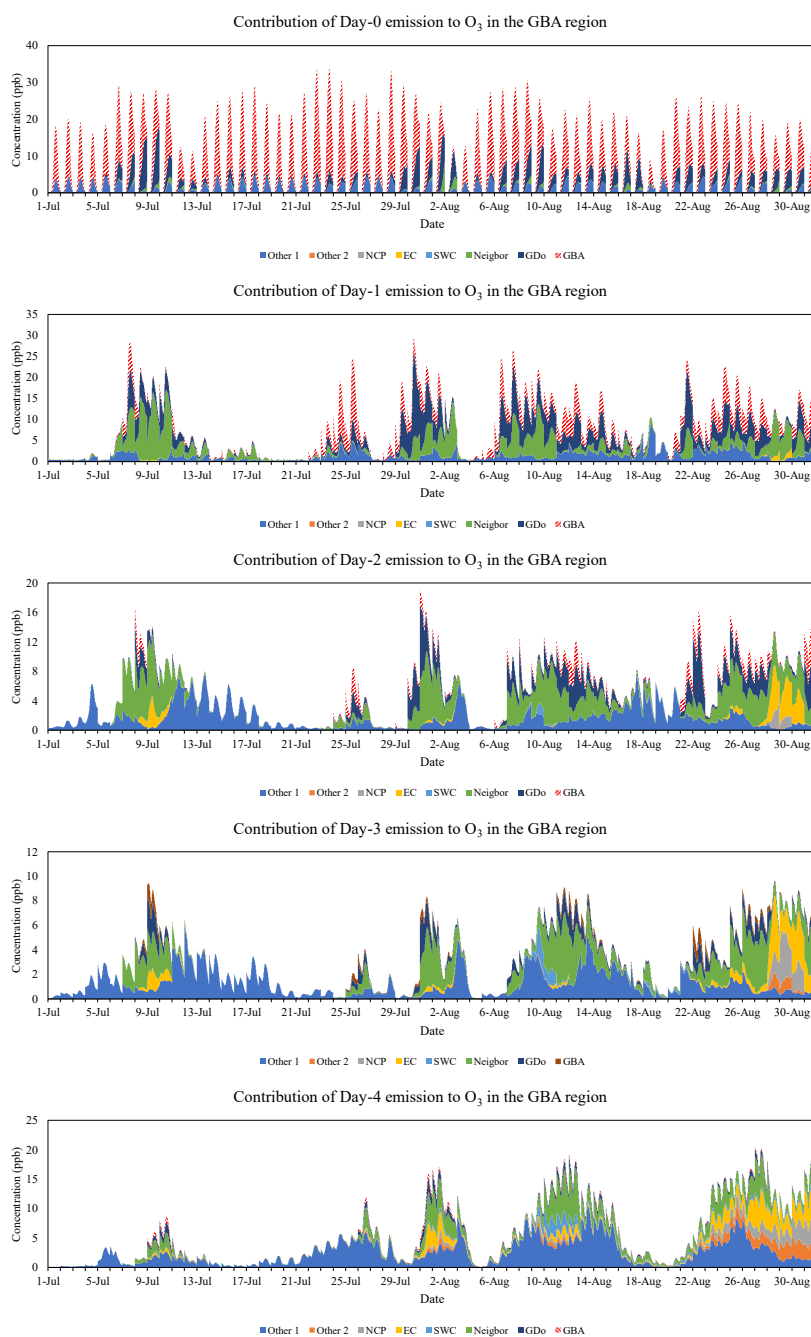
338 On the other hand, the situation is different for the Ep2 ozone pollution. Under the control of high-pressure system
339 and weak southerly wind (Figure S5), the major contributors were mainly the pollutants from the GBA and the
340 ocean. Unlike the Ep1 and Ep3, the pollutant emitted within the GBA still dominant in the Day-1's emission
341 contribution. Under the influence of southerly wind, there is no large amount of pollutants migration from north
342 inland to the GBA and the local pollutants were slowly moving out the GBA. Thus, the pollutant emitted earlier
343 than 2 days ago (\geq Day-2) have a smaller contribution. As shown in Figure 8, the overall diffusion of pollutants
344 within the Guangdong province is much slower during Ep2. The contribution of GBA emissions can still reach
345 more than 10 ppb in the Day-1 emission. These results indicated that this pollution process was mainly driven by
346 the local pollutants within the current 2 days. Hence, emission control should focus on the local sources, and 1-2
347 days in advance is more efficient.

348 For the last O₃ pollution process (Ep4), from the 21st to 25th August, the eastern and southern China were mainly
349 control by the sub-tropical high-pressure system. At the same time, under the joint influence of peripheral
350 subsidence airflow of typhoon, the wind speed over this region was slow (Figure S7). The weak wind not only
351 trapped the O₃ formed local emission but also the O₃ formed from cross-regional transported pollutants. The
352 pollutants from GBA sources mainly dominated the Day-0 and Day-1 emission's contribution, while Day-2 and
353 Day-3 emissions mainly consisted of pollutants from GDo and neighboring provinces. After that, the typhoon
354 moved northerly and the stronger northerly wind further broaden the source areas of the O₃ in the GBA (Figure S7).



355 The major contributor of Day-2 and earlier periods' emission changed to pollutants from the EC and NCP regions.
356 The pollutants emitted earlier than 2 days ago from EC have an important contribution, which accounted for about
357 12%. Furthermore, the pollutants emitted 3 days ago from the North China Plain (NCP) can also have an obvious
358 impact on O₃ over the GBA from July 28th- 30th, which can be up to 10%. Hence, to prevent the occurrence of this
359 pollution, the emission control region should be further broadened and continuously implemented as it lasted for
360 a longer period compared with the other three pollutions.

361 Figure S8 shows the time series of the contributions from different source areas and precursors emission periods
362 for the average O₃ concentration in the GF region and HK city. GF region is located at the inland of the GBA. It
363 is the emission hotspot of the GBA with higher O₃ concentration (Chen et al., 2022a). HK city located at the mouth
364 of the PRD. According to previous source apportionment studies (Li et al., 2012, 2013), the pollution in HK city
365 is more attributed to the emissions outside the GBA compared to the other cities of the GBA. Regarding the O₃ in
366 GF region, Day-0 emission was usually contributed by the local emission and the regional transport within the
367 GBA, which have a similar contribution. The major source areas of the Day-2 to Day-4 emissions contributing to
368 the O₃ in GF in different episodic cases varied similarly to the ones contributing to the average O₃ in the GBA.
369 Generally, the influence of local and GBA regional pollutants to O₃ in the GF region decreased quickly within 1
370 day. However, the regional emission can still have important contribution in the episodic case that southerly wind
371 blew, such as the 24th-25th July (about 26%) in the Ep2 and 23rd-25th (about 15%) in the Ep4. For the O₃ in HK
372 city, the local emission amount is low, and its impact is also limited to the current day. In addition, the O₃ in HK
373 city is also susceptible to the impact of pollutants from the ocean but less from the GBA regional emissions.
374 During the Ep1 periods, it was observed that the contribution of the GBA regional source largely increased in the
375 Day-0 emission as the prevailing wind direction shifted to north. On the other hand, neighboring provinces'
376 emissions dominate the contribution of emissions from Day-1 to Day-3. Unlike the GF region, the influence of
377 EC emission on the O₃ in HK is also limited in Ep1. Similar conclusions can be drawn for the evolution of the
378 spatiotemporal contribution of emission in Ep3. As discussed above, the O₃ pollution in Ep2 is mainly driven by
379 local emissions. Thus, the O₃ concentration in HK city, which is in the upwind region with small local emissions,
380 is much lower than the O₃ concentration in the GF region. In Ep4, same as the GBA average and GF region, the
381 impact of pollutants from EC and NCP became important in the Day-2 and Day-3 emissions, which can contribute
382 up to 20% of O₃. These results indicate that although O₃ is usually a regional pollution problem, it's necessary to
383 consider the local characteristics of different sub-regions while making more specific prevention and control
384 policies.

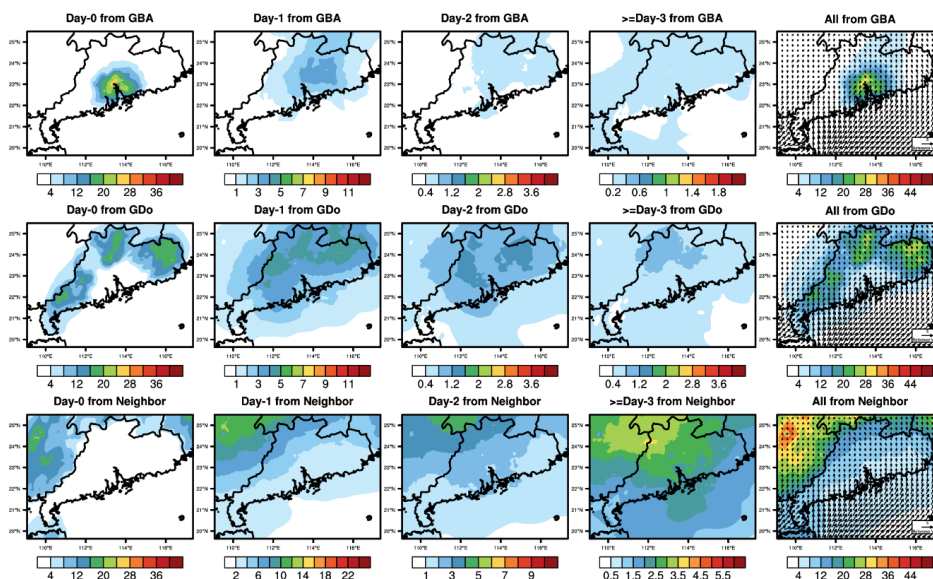


385

386 Figure 5. Time series of contributions from different source areas and emitting periods to the O_3 concentrations in
387 the GBA. (*GDo* represents areas outside the GBA region but within Guangdong province. *Neighbor* represents
388 the provinces around Guangdong province. *Other 1* represents ocean and other countries. *Other 2* represents other
389 area within the mainland China in the simulation domain.)



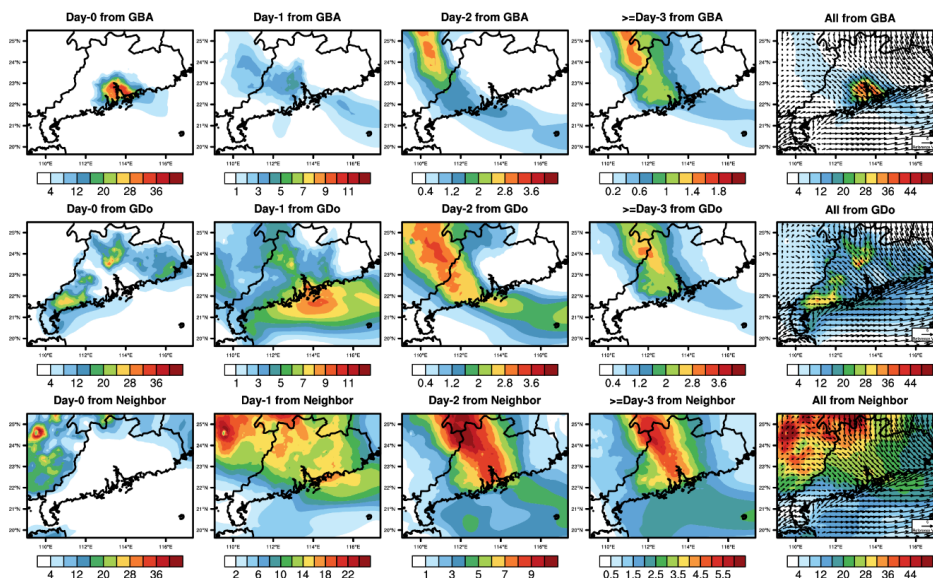
Monthly Average O₃ concentration (ppb)



390

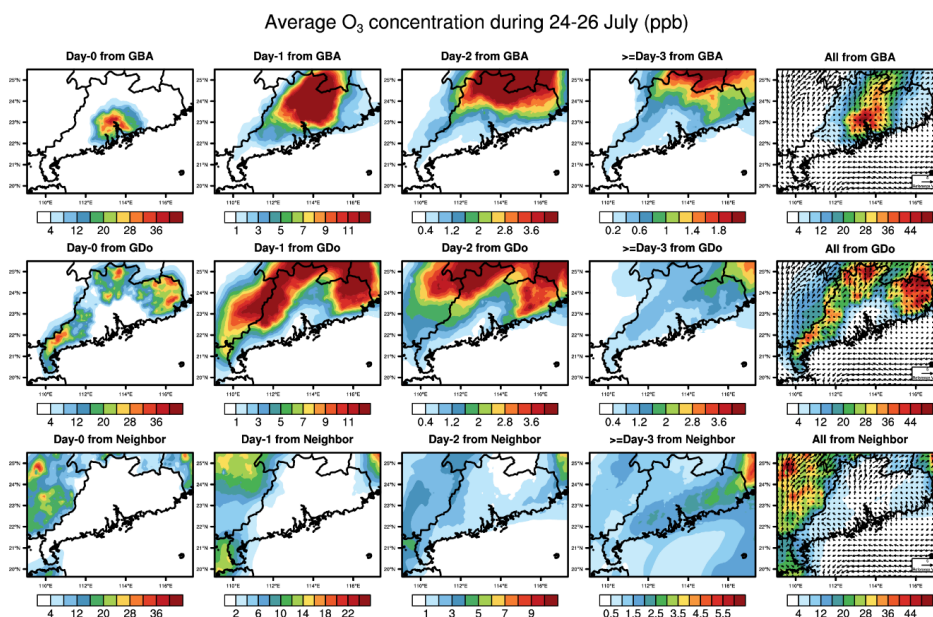
391 Figure 6. Spatial distribution of monthly average O₃ concentration between 9:00-17:00 (Local time) contributed
392 by emission of GBA, other regions within Guangdong province (GDo), and neighboring provinces (Neighbor)
393 from various periods. (Unit: ppb. Due to the large variation of contribution, the colorbar range of each sub-figure
394 is different)

Average O₃ concentration during 7-10 July (ppb)



395

396 Figure 7. Spatial distribution of average O₃ concentration between 9:00-17:00 (Local time) on 7th-10th July 2016
397 contributed by emission of GBA, other regions within Guangdong province (GDo), and neighboring provinces
398 (Neighbor) from various periods. (Unit:ppb. The colorbar range of each sub-figure is same as the one in Figure 6)



399

400 Figure 8. Spatial distribution of average O₃ concentration between 9:00-17:00 (Local time) on 24th-26th July 2016
401 contributed by emission of GBA, other regions within Guangdong province (GDo), and neighboring provinces
402 (Neighbor) from various periods. (Unit: ppb. The colorbar range of each sub-figure is same as the one in Figure
403 6)

404

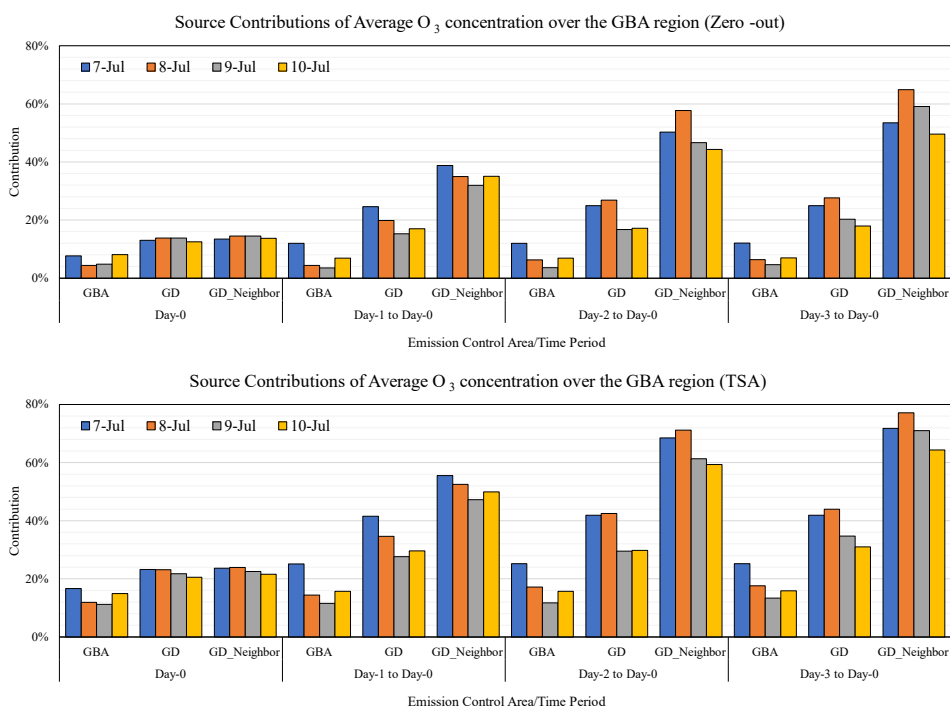
405 3.4 Verification of the TSA by comparing to Zero-out Experiments

406 Here, the emission zero-out sensitivity experiments, another commonly used source apportionment method, were
407 also conducted to evaluate the result from the TSA method. The zero-out method need to conduct two sets of
408 simulation including the control run and zero-out run. In the control run, the simulations were conducted using
409 the complete emissions. In the zero-out runs, the simulations were conducted with the emissions that specific
410 period and area were removed. After that, the contribution of the specific source area and source time was derived
411 by calculating the difference between the control and zero-out simulations. For each target date, the emission
412 control area was set as the GBA, Guangdong province (GD), Guangdong and neighboring provinces
413 (GD_Neighbor), respectively. The emission control period was set as continuous control beginning from the
414 current day, which is also the target day (Day-0), from 1 day ago (Day-1), from 2 days ago (Day-2) and from 3 days
415 ago (Day-3), respectively. The zero-out experiments were carried out for the periods between 7th and 10th July
416 (Typhoon case) and between 24th and 26th (Sub-tropical high case). More configurations can be found in Tables
417 S4- S5.

418 From the result of zero-out experiments (Fig.9 and Fig.S9), it can be seen that, for the typhoon case (Fig.9), when
419 only controlling the emission within the GBA, there is little difference between results of controlling emission 1
420 day in advance and 3 days in advance. This is consistent with the TSA result that the influence of the emission
421 within the GBA is usually limited to 2 days. The effect of controlling emission 1 day ahead in GD is better than
422 that of only GBA. There is less variation of the O₃ concentration when controlling the emission within Guangdong
423 province 2 days and 3 days in advance. Meanwhile, regarding only emission control from the Day-0, it shows
424 limited improvement in controlling the emission for a larger area (GD and GD_neigh) than solely within GBA.
425 It's the same as the TSA result that the pollutants from neighboring provinces took effect on the O₃ over the GBA
426 region at least 1 day later. Joint control from Guangdong and neighboring province (GD_neighbor) has a larger
427 optimal effect in the Day-2 to Day-0 and Day-3 to Day-0 simulations. And the difference between GD_neighbor
428 and the GD result is also more obvious in these simulations, indicating that it's more effective to implement joint
429 control within other provinces 2-3 days in advance.



430 For the sub-tropical high case (Fig.S9), whatever controlling the emission in the current day or 2 days ahead, the
431 effect of only controlling emission within GBA is similar to that of joint controlling larger area (GD and
432 GD_neighbor). It supports our previous conclusion that the pollution is mainly contributed by the local source. At the
433 same time, there is limited optimization effect to control the emission 2-3 days in advance than controlling 1 days
434 in advance. To alleviate this ozone pollution, controlling the local emission within short-term should be effective.
435 Although the contribution discrepancies between the source contribution (%) calculated from the zero-out method
436 and the one from the TSA method can reach 20%, which is due to the non-linear chemistry relationship between
437 ozone and its precursors and the mechanism of different methods (Kwok et al., 2015; Clappier et al., 2017), similar
438 relationships between source area/time and receptor can be drawn. These results also support the validity of the
439 TSA approach.



440

441 Figure 9. The contribution of different source areas and time periods to the O₃ concentration over the GBA in the
442 typhoon case using the zero-out and TSA methods. (Different colors represent different target dates; Upper: Zero-
443 out; Bottom: TSA)

444

445 3.5 Discussion

446 Previous studies mainly focused on exploring the contribution and control of various source areas and categories
447 on O₃ over the GBA. The analysis in this study illustrated that there could be a larger difference between the
448 temporal contribution of emissions to the O₃ pollution over the GBA under different weather patterns. It indicates
449 that understanding the contribution of pollutants from different emitting periods and finding out the major period
450 is also crucial in control policymaking, especially in episodic cases. Different from the zero-out method that needs
451 sets of simulations, it can provide an overall picture of source contributions within one simulation, saving more
452 computation costs, and is suitable for applications in which more potential sources are considered.

453 In addition, meteorological conditions play an important role in affecting the effectiveness of the emission control
454 area and period. The results here suggest that the approach of typhoons usually strengthens the cross-region
455 transportation of pollutants to the GBA. Therefore, cross-province collaboration and control should be



456 implemented at least 2-3 days ahead when the typhoon is predicted. In contrast, local emission control within 2
457 days is more effective when the GBA is under the influence of a high-pressure system. Our findings emphasize
458 the importance of considering the impact of meteorological conditions when implementing control measures in
459 advance. The TSA method could help to better understand the spatial-temporal sources of O₃ pollution under the
460 current emission level. It will provide scientific references for designing of effective and timely control policies
461 when unfavorable weather conditions are predicted. So, the spatial-temporal influence of emission to O₃ over the
462 GBA under other unfavourable conditions and seasons is also essential to further explore through the TSA method,
463 which help to gain a more comprehensive understanding of when and where the O₃ over the GBA comes from.

464 Under the background of climate change, extreme weather, such as extreme heatwaves (Coffel et al., 2018; Dong
465 et al., 2023), may occur more frequently, which will largely impact the source and sink of pollutants by different
466 physical and chemical processes. At the same time, various emission control strategies responding to climate
467 change, such as carbon neutrality (Liu et al., 2021; Zhang et al., 2021), will be implemented by governments in
468 different countries, which will also change the structure of emissions. How these extreme weather and control
469 measures influence the temporal characterization of sources and formation of air pollution, as well as the spatial-
470 temporal contribution of emissions from different countries and their interactions, are also worth further
471 investigation in the future. It can promote the mutual cooperation among nations to combat the environmental
472 issues together.

473 However, it should be noted that the numerical model source apportionment results are usually influenced by the
474 uncertainties of the emission inventory as most of the emission inventories are built up by the bottom-up method
475 and cannot be updated in a timely manner. With the increasing availability of different types of observations,
476 including surface monitoring and satellite remote sensing data, different top-down methods such as data
477 assimilation (East et al., 2022) and machine learning (Chen et al., 2023) have been applied to integrate
478 observations and optimize the emission. These methods should be implemented to update the emission inventory
479 and combined with the TSA method to evaluate the evolution of spatial-temporal sources in different historical
480 periods and provide up-to-date source information for policymaking.

481

482 **4. Conclusion**

483 In this study, we applied the CAMx-TSA method to analyze the spatial and temporal contribution of different
484 sources to the O₃ pollution in the GBA in summer. The result shows that the O₃ over the GBA in summer is mainly
485 contributed by the pollutants from local emissions, followed by other regions within Guangdong province (GDo)
486 and neighbouring provinces. The O₃ was usually formed by the pollutants emitted within 3days, which account
487 for more than 70%. During the O₃ episodes, when the typhoon moved from the eastern Philippine Sea to southern
488 China, the prevailing wind shifted from south to north over the GBA. It conducive more pollutants transported
489 from GDo and neighbouring provinces to the GBA, leading to an increase in O₃ concentrations. The pollutants
490 emitted 3 days ago still have a significant contribution. While the typhoon just stayed near the sea areas east of
491 Taiwan province and moved northly, under the continuous influence of northly wind, the emission of eastern
492 China, even the North China Plain from 3 days ago can also have an obvious impact on O₃ over the GBA. In
493 contrast, when the GBA is mainly under the control of sub-tropical high-pressure system, the ozone pollution was
494 mainly caused by the local pollutants within the current 2 days. The results indicated that joint emission control
495 action with other provinces 2-3 days in advance is more effective for preventing the O₃ pollution in the GBA when
496 the typhoon is moving towards southern China. On the other hand, it's more efficient to pay more attention to
497 local sources control within 2 days when the GBA is under the control of the high-pressure system.

498 Here, different surrounding provinces were categorized as one source area here to save computation resource for
499 more potential source investigation. As the neighbouring province was illustrated as a major contributor to the O₃
500 in the GBA, it is necessary to further divided this source into several sub-source areas and explore their individual
501 impact in future work. In addition, individual source categories were not separated in this study, mainly due to the
502 application of different emission inventories with different source category classifications, making it difficult to
503 combine them. It is important to note that each source category has its own characteristic temporal profile, which
504 can have different temporal impacts on O₃ concentrations. Therefore, the temporal contribution of various source
505 categories, including anthropogenic and biogenic emissions, should be also considered in future work. These
506 works can provide more spatial and temporal information of O₃ source over the GBA to the local governments so
507 that the targeted control measures can be designed and implemented more effectively and timely.



508

509 **Code and Data availability**

510 Hourly O₃ observation data were released by the China National Environmental Monitoring Centre
511 (<http://www.cnemc.cn/en>, last access 24 December; CNEMC, 2023) and the Hong Kong Environmental
512 Protection Department (<https://cd.epic.epd.gov.hk/EPICDI/air/station/?lang=en>, last access 24 December 2023;
513 HKEPD, 2023). The CAMx model code is freely available via <https://www.camx.com/download/>, last access 24
514 December, 2023)

515

516 **Author contribution**

517 CY, LX, and JF designed the research. CY contributed to model development, simulation and data analysis. LX
518 and JF contributed to the result discussion. CY prepared the manuscript with contributions from all co-authors.

519

520 **Competing interests**

521 The authors declare that they have no conflict of interest.

522

523 **Acknowledgements**

524 This work was supported by the Research Grants Council of Hong Kong Government (C6026-22GF) and the
525 Improvement on Competitiveness in Hiring New Faculties Funding Scheme of CUHK (No. 4937115)

526

527 **References**

528 Cao, M., Fan, S., Jin, C., Cai, Q., and He, Y.: O₃ pollution characteristics, weather classifications and local
529 meteorological conditions in Guangdong from 2015 to 2020, *Acta Scientiae Circumstantiae*, 43, 19-31,
530 10.13671/j.hjkxxb.2022.0416, 2023. (in Chinese)

531 Cao, T., Wang, H., Li, L., Lu, X., Liu, Y., and Fan, S.: Fast spreading of surface ozone in both temporal and spatial
532 scale in Pearl River Delta, *Journal of Environmental Sciences*, 137, 540-552, 10.1016/j.jes.2023.02.025, 2024.

533 Chen, W., Chen, Y., Chu, Y., Zhang, J., Xian, C., Lin, C., Fung, Z., and Lu, X.: Numerical simulation of ozone
534 source characteristics in the Pearl River Delta region, *Acta Scientiae Circumstantiae*, 42, 293-308,
535 10.13671/j.hjkxxb.2021.0328, 2022a. (in Chinese)

536 Chen, X., Wang, N., Wang, G., Wang, Z., Chen, H., Cheng, C., Li, M., Zheng, L., Wu, L., Zhang, Q., Tang, M.,
537 Huang, B., Wang, X., and Zhou, Z.: The Influence of Synoptic Weather Patterns on Spatiotemporal Characteristics
538 of Ozone Pollution Across Pearl River Delta of Southern China, *Journal of Geophysical Research: Atmospheres*,
539 127, 10.1029/2022jd037121, 2022b.

540 Chen, Y., Fung, J. C. H., Huang, Y., Lu, X., Wang, Z., Louie, P. K. K., Chen, W., Yu, C. W., Yu, R., and Lau, A. K.
541 H.: Temporal Source Apportionment of PM_{2.5} Over the Pearl River Delta Region in Southern China, *Journal of*
542 *Geophysical Research: Atmospheres*, 127, 10.1029/2021jd035271, 2022c.

543 Chen, Y., Fung, J. C. H., Yuan, D., Chen, W., Fung, T., and Lu, X.: Development of an integrated machine-learning
544 and data assimilation framework for NO_x emission inversion, *Science of The Total Environment*, 871,
545 10.1016/j.scitotenv.2023.161951, 2023.

546 Clappier, A., Belis, C. A., Pernigotti, D., and Thunis, P.: Source apportionment and sensitivity analysis: two
547 methodologies with two different purposes, *Geoscientific Model Development*, 10, 4245-4256, 10.5194/gmd-10-
548 4245-2017, 2017.



- 549 CNEMC: China National Environmental Monitoring Centre: Real-time National Air Quality,
550 <http://www.cnemc.cn/en>, last access: 24 December 2023.
- 551 Coffel, E. D., Horton, R. M., and de Sherbinin, A.: Temperature and humidity based projections of a rapid rise in
552 global heat stress exposure during the 21st century, *Environmental Research Letters*, 13, 10.1088/1748-
553 9326/aaa00e, 2018.
- 554 Deng, T., Wang, T., Wang, S., Zou, Y., Yin, C., Li, F., Liu, L., Wang, N., Song, L., Wu, C., and Wu, D.: Impact of
555 typhoon periphery on high ozone and high aerosol pollution in the Pearl River Delta region, *Science of The Total
556 Environment*, 668, 617-630, 10.1016/j.scitotenv.2019.02.450, 2019.
- 557 Dong, W., Jia, X., Qian, Q., and Li, X.: Rapid Acceleration of Dangerous Compound Heatwaves and Their Impacts
558 in a Warmer China, *Geophysical Research Letters*, 50, 10.1029/2023gl104850, 2023.
- 559 East, J. D., Henderson, B. H., Napelenok, S. L., Koplitz, S. N., Sarwar, G., Gilliam, R., Lenzen, A., Tong, D. Q.,
560 Pierce, R. B., and Garcia-Menendez, F.: Inferring and evaluating satellite-based constraints on NO_x emissions
561 estimates in air quality simulations, *Atmospheric Chemistry and Physics*, 22, 15981-16001, 10.5194/acp-22-
562 15981-2022, 2022.
- 563 Emery, C., Tai, E., and Yarwood, G.: Enhanced meteorological modeling and performance evaluation for two
564 Texas ozone episodes, Prepared for the Texas natural resource conservation commission, by ENVIRON
565 International Corporation, 2001.
- 566 EPA, U.: Guidance on the use of models and other analyses for demonstrating attainment of air quality goals for
567 ozone, PM_{2.5}, and regional haze, Technical Support Document, 2007.
- 568 Fang, T., Zhu, Y., Wang, S., Xing, J., Zhao, B., Fan, S., Li, M., Yang, W., Chen, Y., and Huang, R.: Source impact
569 and contribution analysis of ambient ozone using multi-modeling approaches over the Pearl River Delta region,
570 *China, Environmental Pollution*, 289, 10.1016/j.envpol.2021.117860, 2021.
- 571 Feng, X., Guo, J., Wang, Z., Gu, D., Ho, K.-F., Chen, Y., Liao, K., Cheung, V. T. F., Louie, P. K. K., Leung, K. K.
572 M., Yu, J. Z., Fung, J. C. H., and Lau, A. K. H.: Investigation of the multi-year trend of surface ozone and ozone-
573 precursor relationship in Hong Kong, *Atmospheric Environment*, 315, 10.1016/j.atmosenv.2023.120139, 2023.
- 574 Gao, X., Deng, X., Tan, H., Wang, C., Wang, N., and Yue, D.: Characteristics and analysis on regional pollution
575 process and circulation weather types over Guangdong Province, *Acta Scientiae Circumstantiae*, 38, 1708-1716,
576 10.13671/j.hjkxxb.2017.0473, 2018. (in Chinese)
- 577 Gong, C., Liao, H., Yue, X., Ma, Y., and Lei, Y.: Impacts of Ozone-Vegetation Interactions on Ozone Pollution
578 Episodes in North China and the Yangtze River Delta, *Geophysical Research Letters*, 48, 10.1029/2021gl093814,
579 2021.
- 580 Gong, S., Zhang, L., Liu, C., Lu, S., Pan, W., and Zhang, Y.: Multi-scale analysis of the impacts of meteorology
581 and emissions on PM_{2.5} and O₃ trends at various regions in China from 2013 to 2020 2. Key weather elements and
582 emissions, *Science of The Total Environment*, 824, 10.1016/j.scitotenv.2022.153847, 2022.
- 583 Han, H., Liu, J., Shu, L., Wang, T., and Yuan, H.: Local and synoptic meteorological influences on daily variability
584 in summertime surface ozone in eastern China, *Atmospheric Chemistry and Physics*, 20, 203-222, 10.5194/acp-
585 20-203-2020, 2020.
- 586 He, Z., Wang, X., Ling, Z., Zhao, J., Guo, H., Shao, M., and Wang, Z.: Contributions of different anthropogenic
587 volatile organic compound sources to ozone formation at a receptor site in the Pearl River Delta region and its
588 policy implications, *Atmospheric Chemistry and Physics*, 19, 8801-8816, 10.5194/acp-19-8801-2019, 2019.
- 589 HKPD, Hong Kong Air Quality Data, <https://cd.epic.epd.gov.hk/EPICDI/air/station/?lang=en>, last access: 24
590 December 2023)
- 591 Kwok, R., Baker, K., Napelenok, S., and Tonnesen, G.: Photochemical grid model implementation and application
592 of VOC, NO_x, and O₃ source apportionment, *Geoscientific Model Development*, 8, 99-114, 2015.



- 593 Li, M., Liu, H., Geng, G., Hong, C., Liu, F., Song, Y., Tong, D., Zheng, B., Cui, H., Man, H., Zhang, Q., and He,
594 K.: Anthropogenic emission inventories in China: a review, *National Science Review*, 4, 834-866,
595 10.1093/nsr/nwx150, 2017.
- 596 Li, Y., Lau, A. K. H., Fung, J. C. H., Zheng, J. Y., Zhong, L. J., and Louie, P. K. K.: Ozone source apportionment
597 (OSAT) to differentiate local regional and super-regional source contributions in the Pearl River Delta region,
598 China, *Journal of Geophysical Research: Atmospheres*, 117, 10.1029/2011jd017340, 2012.
- 599 Li, Y., Lau, A. K. H., Fung, J. C. H., Ma, H., and Tse, Y.: Systematic evaluation of ozone control policies using an
600 Ozone Source Apportionment method, *Atmospheric Environment*, 76, 136-146, 10.1016/j.atmosenv.2013.02.033,
601 2013.
- 602 Li, Y., Zhao, X., Deng, X., and Gao, J.: The impact of peripheral circulation characteristics of typhoon on sustained
603 ozone episodes over the Pearl River Delta region, China, *Atmospheric Chemistry and Physics*, 22, 3861-3873,
604 10.5194/acp-22-3861-2022, 2022.
- 605 Lin, X., Yuan, Z., Yang, L., Luo, H., and Li, W.: Impact of Extreme Meteorological Events on Ozone in the Pearl
606 River Delta, China, *Aerosol and Air Quality Research*, 19, 1307-1324, 10.4209/aaqr.2019.01.0027, 2019.
- 607 Liu, H., Zhang, M., and Han, X.: A review of surface ozone source apportionment in China, *Atmospheric and
608 Oceanic Science Letters*, 13, 470-484, 10.1080/16742834.2020.1768025, 2020a.
- 609 Liu, Y. and Wang, T.: Worsening urban ozone pollution in China from 2013 to 2017 – Part 1: The complex and
610 varying roles of meteorology, *Atmospheric Chemistry and Physics*, 20, 6305-6321, 10.5194/acp-20-6305-2020,
611 2020b.
- 612 Liu, Y., Geng, G., Cheng, J., Liu, Y., Xiao, Q., Liu, L., Shi, Q., Tong, D., He, K., and Zhang, Q.: Drivers of
613 Increasing Ozone during the Two Phases of Clean Air Actions in China 2013–2020, *Environmental Science &
614 Technology*, 57, 8954-8964, 10.1021/acs.est.3c00054, 2023.
- 615
- 616 Liu, Z., Deng, Z., He, G., Wang, H., Zhang, X., Lin, J., Qi, Y., and Liang, X.: Challenges and opportunities for
617 carbon neutrality in China, *Nature Reviews Earth & Environment*, 3, 141-155, 10.1038/s43017-021-00244-x,
618 2021.
- 619 Lu, X., Yao, T., Li, Y., Fung, J. C. H., and Lau, A. K. H.: Source apportionment and health effect of NO_x over the
620 Pearl River Delta region in southern China, *Environmental Pollution*, 212, 135-146,
621 10.1016/j.envpol.2016.01.056, 2016.
- 622 Lu, X., Zhang, L., and Shen, L.: Meteorology and Climate Influences on Tropospheric Ozone: a Review of Natural
623 Sources, Chemistry, and Transport Patterns, *Current Pollution Reports*, 5, 238-260, 10.1007/s40726-019-00118-
624 3, 2019.
- 625 Maji, K. J., Ye, W.-F., Arora, M., and Nagendra, S. M. S.: Ozone pollution in Chinese cities: Assessment of
626 seasonal variation, health effects and economic burden, *Environmental Pollution*, 247, 792-801,
627 10.1016/j.envpol.2019.01.049, 2019.
- 628 Ouyang, S., Deng, T., Liu, R., Chen, J., He, G., Leung, J. C.-H., Wang, N., and Liu, S. C.: Impact of a subtropical
629 high and a typhoon on a severe ozone pollution episode in the Pearl River Delta, China, *Atmospheric Chemistry
630 and Physics*, 22, 10751-10767, 10.5194/acp-22-10751-2022, 2022.
- 631 Qu, K., Wang, X., Yan, Y., Shen, J., Xiao, T., Dong, H., Zeng, L., and Zhang, Y.: A comparative study to reveal
632 the influence of typhoons on the transport, production and accumulation of O₃ in the Pearl River Delta, China,
633 *Atmospheric Chemistry and Physics*, 21, 11593-11612, 10.5194/acp-21-11593-2021, 2021.
- 634 Sahu, S. K., Liu, S., Liu, S., Ding, D., and Xing, J.: Ozone pollution in China: Background and transboundary
635 contributions to ozone concentration & related health effects across the country, *Science of The Total Environment*,
636 761, 10.1016/j.scitotenv.2020.144131, 2021.



- 637 Wang, N., Huang, X., Xu, J., Wang, T., Tan, Z.-m., and Ding, A.: Typhoon-boosted biogenic emission aggravates
638 cross-regional ozone pollution in China, *Science Advances*, 8, eabl6166, 2022a.
- 639 Wang, T., Xue, L., Brimblecombe, P., Lam, Y. F., Li, L., and Zhang, L.: Ozone pollution in China: A review of
640 concentrations, meteorological influences, chemical precursors, and effects, *Science of The Total Environment*,
641 575, 1582-1596, 10.1016/j.scitotenv.2016.10.081, 2017.
- 642 Wang, T., Xue, L., Feng, Z., Dai, J., Zhang, Y., and Tan, Y.: Ground-level ozone pollution in China: a synthesis of
643 recent findings on influencing factors and impacts, *Environmental Research Letters*, 17, 10.1088/1748-
644 9326/ac69fe, 2022b.
- 645 Wang, Y., Wild, O., Ashworth, K., Chen, X., Wu, Q., Qi, Y., and Wang, Z.: Reductions in crop yields across China
646 from elevated ozone, *Environmental Pollution*, 292, 10.1016/j.envpol.2021.118218, 2022c.
- 647 Wu, Y., Chen, W., You, Y., Xie, Q., Jia, S., and Wang, X.: Quantitative impacts of vertical transport on the long-
648 term trend of nocturnal ozone increase over the Pearl River Delta region during 2006–2019, *Atmospheric
649 Chemistry and Physics*, 23, 453-469, 10.5194/acp-23-453-2023, 2023.
- 650 Xie, X., Shi, Z., Ying, Q., Zhang, H., and Hu, J.: Age-Resolved Source and Region Contributions to Fine
651 Particulate Matter During an Extreme Haze Episode in China, *Geophysical Research Letters*, 48,
652 10.1029/2021gl095388, 2021.
- 653 Xie, X., Hu, J., Qin, M., Guo, S., Hu, M., Ji, D., Wang, H., Lou, S., Huang, C., Liu, C., Zhang, H., Ying, Q., Liao,
654 H., and Zhang, Y.: Evolution of atmospheric age of particles and its implications for the formation of a severe
655 haze event in eastern China, *Atmospheric Chemistry and Physics*, 23, 10563-10578, 10.5194/acp-23-10563-2023,
656 2023.
- 657 Xu, J., Zhao, Z., Wu, Y., Zhang, Y., Wang, Y., Su, B., Liang, Y., Hu, T., and Liu, R.: Impacts of Meteorological
658 Conditions on Autumn Surface Ozone During 2014–2020 in the Pearl River Delta, China, *Earth and Space Science*,
659 10, 10.1029/2022ea002742, 2023a.
- 660 Xu, Y., Shen, A., Jin, Y., Liu, Y., Lu, X., Fan, S., Hong, Y., and Fan, Q.: A quantitative assessment and process
661 analysis of the contribution from meteorological conditions in an O₃ pollution episode in Guangzhou, China,
662 *Atmospheric Environment*, 303, 10.1016/j.atmosenv.2023.119757, 2023b.
- 663 Yang, J. and Zhao, Y.: Performance and application of air quality models on ozone simulation in China – A review,
664 *Atmospheric Environment*, 293, 10.1016/j.atmosenv.2022.119446, 2023.
- 665 Yang, L., Luo, H., Yuan, Z., Zheng, J., Huang, Z., Li, C., Lin, X., Louie, P. K. K., Chen, D., and Bian, Y.:
666 Quantitative impacts of meteorology and precursor emission changes on the long-term trend of ambient ozone
667 over the Pearl River Delta, China, and implications for ozone control strategy, *Atmospheric Chemistry and Physics*,
668 19, 12901-12916, 10.5194/acp-19-12901-2019, 2019a.
- 669 Yang, W., Chen, H., Wang, W., Wu, J., Li, J., Wang, Z., Zheng, J., and Chen, D.: Modeling study of ozone source
670 apportionment over the Pearl River Delta in 2015, *Environmental Pollution*, 253, 393-402,
671 10.1016/j.envpol.2019.06.091, 2019b.
- 672 Yin, P., Chen, R., Wang, L., Meng, X., Liu, C., Niu, Y., Lin, Z., Liu, Y., Liu, J., Qi, J., You, J., Zhou, M., and Kan,
673 H.: Ambient Ozone Pollution and Daily Mortality: A Nationwide Study in 272 Chinese Cities, *Environmental
674 Health Perspectives*, 125, 10.1289/ehp1849, 2017.
- 675 Ying, Q., Zhang, J., Zhang, H., Hu, J., and Kleeman, M. J.: Atmospheric Age Distribution of Primary and
676 Secondary Inorganic Aerosols in a Polluted Atmosphere, *Environmental Science & Technology*, 55, 5668-5676,
677 10.1021/acs.est.0c07334, 2021.
- 678 Zeren, Y., Zhou, B., Zheng, Y., Jiang, F., Lyu, X., Xue, L., Wang, H., Liu, X., and Guo, H.: Does Ozone Pollution
679 Share the Same Formation Mechanisms in the Bay Areas of China?, *Environmental Science & Technology*, 56,
680 14326-14337, 10.1021/acs.est.2c05126, 2022.



- 681 Zhang, R. and Hanaoka, T.: Deployment of electric vehicles in China to meet the carbon neutral target by 2060:
682 Provincial disparities in energy systems, CO₂ emissions, and cost effectiveness, *Resources, Conservation and*
683 *Recycling*, 170, 10.1016/j.resconrec.2021.105622, 2021.
- 684 Zheng, H., Kong, S., He, Y., Song, C., Cheng, Y., Yao, L., Chen, N., and Zhu, B.: Enhanced ozone pollution in the
685 summer of 2022 in China: The roles of meteorology and emission variations, *Atmospheric Environment*, 301,
686 10.1016/j.atmosenv.2023.119701, 2023.
- 687